Title

Quantitative Mass Spectrometry Analysis of Cerebrospinal Fluid Protein Biomarkers in Alzheimer's Disease

Authors

Caroline M. Watson[1], Eric B. Dammer[1], Lingyan Ping[1], Duc M. Duong[2], Erica Modeste[1], E. Kathleen Carter[2], Erik C. B. Johnson[1], Allan I. Levey[1*], James J. Lah[1*], Blaine R. Roberts[1,2], and Nicholas T. Seyfried[1,2*]

Affiliations

1. Department of Neurology, Emory University School of Medicine
2. Department of Biochemistry, Emory University School of Medicine

corresponding author(s): Nicholas T. Seyfried, PhD (nseyfri@emory.edu); James J. Lah, MD, PhD. (jlah@emory.edu); Allan I Levey, MD, PhD. (alevey@emory.edu)

Abstract

Alzheimer's disease (AD) is the most common form of dementia, with cerebrospinal fluid (CSF) β-amyloid (Aβ), total Tau, and phosphorylated Tau providing the most sensitive and specific biomarkers for diagnosis. However, these diagnostic biomarkers do not reflect the complex changes in AD brain beyond amyloid (A) and Tau (T) pathologies. Here, we report a selected reaction monitoring mass spectrometry (SRM-MS) method with isotopically labeled standards for relative protein quantification in CSF. Biomarker positive (AT+) and negative (AT-) CSF pools were used as quality controls (QCs) to assess assay precision. We detected 62 peptides (51 proteins) with an average CV of ~13% across 30 QCs and 133 controls (cognitively normal, AT), 127 asymptomatic (cognitively normal, AT+) and 130 symptomatic AD (cognitively impaired, AT+). Proteins that could distinguish AT+ from AT- individuals included SMOC1, GDA, 14-3-3 proteins, and those involved in glycolysis. Proteins that could distinguish cognitive impairment were mainly neuronal proteins (VGF, NPTX2, NPTXR, and SCG2). This demonstrates the utility of SRM-MS to quantify CSF protein biomarkers across stages of AD.

Background & Summary

Alzheimer's disease (AD) affects more than 45 million people worldwide, making it the most common neurodegenerative disease[1] (https://www.alz.org/media/Documents/alzheimers-facts-and-figures-2019-r.pdf; https://www.alzint.org/u/WorldAlzheimerReport2015.pdf). AD biomarker research has predominately focused on β-amyloid (Aβ) and Tau, as these proteins reflect pathological Aβ plaques and tau neurofibrillary tangles (NFT), respectively, in AD[2,3]. Although Aβ and Tau are the most sensitive and specific CSF biomarkers for diagnosis[4,5] these two proteins do not reflect the heterogenous and complex changes in AD brain[6,7]. Furthermore, failed clinical trials of Aβ-based therapeutic approaches highlight the complexity of AD and the need for additional biomarkers to fully illustrate pathophysiology for advancements in diagnostic profiling, disease monitoring, and treatments[1,7] (https://www.alz.org/media/Documents/alzheimers-facts-and-figures-2019-r.pdf; https://www.alzint.org/u/WorldAlzheimerReport2015.pdf).

Considering the diagnostic challenges related to the overlapping pathologies of neurodegenerative diseases, AD biomarkers that represent diverse pathophysiological

changes could facilitate an early diagnosis, predict disease progression, and enhance the understanding of neuropathological changes in AD[1]. AD has a characteristic pre-clinical or asymptomatic period (AsymAD) where individuals have AD neuropathology in the absence of clinical cognitive decline[3,8,9]. Thus, biomarkers for the prodromal phase of AD that can begin changing years or decades before signs of cognitive impairment, would be valuable for disease intervention, clinical trial stratification, and monitoring drug efficacy.

Proteins are the proximate mediators of disease, integrating the effects of genetic, epigenetic, and environmental factors[7,10]. Network proteomic analysis has emerged as a valuable tool for organizing complex unbiased proteomic data into groups or "modules" of co-expressed proteins that reflect various biological functions, i.e., systems biology [11-14]. The direct proximity of CSF to the brain presents a strong rationale to integrate the brain and CSF proteomes to increase the pathophysiological diversity among biofluid biomarkers of AD[5,15]. We recently integrated a human AD brain proteomic network with a CSF proteome differential expression analysis and revealed approximately 70% of the CSF proteome overlapped with the brain proteome[16]. Nearly 300 CSF proteins were identified as significantly altered between control and AD samples, representing predominately neuronal, glial, vasculature and metabolic pathways, creating an excellent list of candidates for further quantification and validation.

Here, we developed a high-throughput targeted selected reaction monitoring-based mass spectrometry (SRM-MS) assay[17] to quantify and validate reliably detected CSF proteins in healthy individuals and individuals with asymptomatic or symptomatic AD for staging AD progression. We evaluated 200+ tryptic peptides that were selected using a data-driven approach from the integrated brain-CSF proteome network analysis. We selected peptides with differential abundance in AD CSF observed in >50 percent of case samples by discovery proteomics[16] for synthesis as crude heavy standards. We used two pooled CSF reference standards to determine which peptides were reliably detected in CSF matrix. We reproducibly detected and reliably quantified 62 tryptic peptides from 51 proteins in 390 clinical samples and 30 pooled reference standards. Furthermore, using a combination of differential expression and receiver operating curve (ROC) analyses we found CSF proteins that can best discriminate stages of AD progression. Collectively, these data highlight the utility of a high throughput SRM-MS approach to quantify biomarkers associated with AD that ultimately hold promise for monitoring disease progression, stratifying patients for clinical trials, and measuring therapeutic response. Future studies will be necessary to assess the diagnostic and predictive utility of our CSF peptide SRM panel against gold-standard CSF (amyloid, tau and pTau) and imaging AD biomarkers in larger prospective patient cohorts.

Methods

Reagents and materials

Heavy labeled peptides (Thermo PEPotec SRM Peptide Libraries; Grade 2; crude as synthesized), trypsin, mass spectrometry grade, trifluoroacetic acid (TFA), foil heat seals (AB-0757), and low-profile square storage plates (AB-1127) were purchased from ThermoFisher Scientific (Waltham, MA). Lysyl endopeptidase (Lys-C), mass spectrometry grade was bought from Wako (Japan); sodium deoxycholate, CAA (chloroacetamide), TCEP (tris-2(-carboxyethyl)-phosphine), and triethylammonium hydrogen carbonate buffer (TEAB) (1 M, pH 8.5) were obtained from Sigma (St. Louis, MO). Formic acid (FA), 0.1% FA in acetonitrile, 0.1% FA in water, methanol, and sample preparation V-bottom plates (Greiner Bio-One 96-well Polypropylene Microplates; 651261) are from Fisher Scientific (Pittsburgh, PA). Oasis PRiME HLB 96-well, 30mg sorbent per well, solid phase extraction (SPE) cleanup plates were from Waters Corporation (Milford, MA).

105
106
107 **Pooled CSF as quality controls**
108 Two pools of CSF were generated based on Aβ(1-42), total Tau, and pTau181 levels to create
109 AD-positive (AT+) and AD-negative (AT-) quality control standards. Each pool consisted of
110 approximately 50 mL of CSF by combining equal volumes of CSF selected from well
111 characterized samples (~45 unique individuals per pool) from the Emory Goizueta Alzheimer's
112 Disease Research Center (GADRC) and Emory Healthy Brain Study (EHBS). All research
113 participants provided informed consent under protocols approved by the Institutional Review
114 Board (IRB) at Emory University. CSF was collected by lumbar puncture and banked according
115 to 2014 ADC/NIA best practices guidelines (https://www.alz.washington.edu/Biospecimen
116 TaskForce.html). AD biomarker status for individual cases was determined on the Roche
117 Elecsys® immunoassay platform[18-20]; the average CSF biomarker value is reported in
118 parentheses. The control CSF pool (AT-) was comprised of cases with relatively high levels of
119 Aβ(1-42) (1457.3 pg/mL) and low total Tau (172.0 pg/mL) and pTau181 (15.1 pg/mL). In
120 contrast, the AD pool (AT+) was comprised of cases with low levels of Aβ(1-42) (482.6 pg/mL)
121 and high total Tau (341.3 pg/mL) and pTau181 (33.1 pg/mL). The quality control (QC) pools
122 were processed and analyzed identically to the CSF clinical samples reported.
123
124 **Clinical characteristics of the cohort**
125 Human cerebrospinal fluid (CSF) samples from 390 individuals including 133 healthy controls,
126 130 patients with symptomatic AD, and 127 asymptomatic AD patients (cognitively normal but
127 AD biomarker positive) were obtained from Emory's GADRC and EHBS (**Fig. 1 and Table 1**). All
128 symptomatic individuals were diagnosed by expert clinicians in the ADRC and Emory Cognitive
129 Neurology Program, who are subspecialty trained in Cognitive and Behavioral Neurology,
130 following extensive clinical evaluations including detailed cognitive testing, neuroimaging, and
131 laboratory studies. CSF samples were selected to balance for age and sex (**Table 1**). For
132 biomarker measurements, CSF samples from all individuals were assayed for Aβ(1-42), total
133 Tau, and pTau using the Roche Diagnostics Elecsys® immunoassay platform[18-20]. The cohort
134 characteristics are summarized in **Fig. 1 and Table 1**. Compared to our previous CSF
135 studies[14,16,21], there is minimal overlap with 329 of the 390 CSF samples (~84%) unique to this
136 study. Samples were stratified into controls, AsymAD, and AD based on Tau and Amyloid
137 biomarkers status and cognitive score from the Montreal Cognitive Assessment (MoCA). All
138 case metadata including disease state, age, sex, race, apolipoprotein (ApoE) genotype, MoCA
139 scores, and biomarkers measurements were deposited on Synapse[22].
140
141 **Peptide selection and selected reaction monitoring assay**
142 We harnessed both deep discovery and single-shot tandem mass tag (ssTMT) peptide data
143 from CSF proteomics[14,16]. Here, we prioritized peptides for SRM validation that i) had one or
144 more spectral match, ii) were differentially abundant (AD versus control) iii) or that mapped
145 to proteins within brain-based biological panels that differed in AD[16]. Ultimately, we
146 nominated 200+ peptides for synthesis as crude heavy standards. The heavy peptides
147 contained isotopically labeled C-terminal lysine or arginine residues (^{13}C, ^{15}N) for each tryptic
148 peptide. Based on the crude heavy peptide signal, the peptides were pooled to achieve total
149 area signals ≥ $1x10^5$ in CSF matrix. The transition lists were created in Skyline-daily software
150 (version 21.2.1.455)[23,24]. An in-house spectral library was created in Skyline based on tandem
151 mass spectra from CSF samples. Skyline parameters were specified as: trypsin enzyme, Swiss-
152 Prot background proteome, and carbamidomethylation of cysteine residues (+57.02146 Da)
153 as fixed modifications. Isotope modifications included: $^{13}C_6{}^{15}N_4$ (C-term R) and $^{13}C_6{}^{15}N_2$ (C-term
154 K). The top ten fragment ions that matched the criteria (precursor charges: 2; ion charges 1,
155 2; ion types: y, b) were selected for scrutiny. The top 5-7 transitions per heavy precursor were
156 selected by manual inspection of the data in Skyline and scheduled transition lists were

created for collision energy optimization. Collision energies were optimized for each transition; the collision energy was ramped around the predicted value in 3 steps on both sides, in 2V increments[25]. The selected transitions were tested in real matrix spiked with the heavy peptide mixtures. The three best transitions per precursor were selected by manual inspection of the data in Skyline and one scheduled transition list was created for the final assays. A list of transitions used in this study is deposited on Synapse[22].

Preparation of CSF for mass spectrometric analysis

All CSF samples were blinded and randomized. Each CSF sample was thawed and aliquoted into sample preparation V-bottom plates that also included quality controls. Each sample and quality control were processed independently in parallel. Crude CSF (50 µL) was reduced, alkylated, and denatured with tris-2(-carboxyethyl)-phosphine (5 mM), chloroacetamide (40 mM), and sodium deoxycholate (1%) in triethylammonium bicarbonate buffer (100 mM) in a final volume of 150 µL. Sample plates were heated at 95°C for 10 min, followed by a 10-min cool down at room temperature while shaking on an orbital shaker (300 rpm)[26]. CSF proteins were digested with Lys-C (Wako; 0.5 µg; 1:100 enzyme to CSF volume) and trypsin (Pierce; 5 µg; 1:10 enzyme to CSF volume) overnight in a 37°C oven. After digestion, heavy labeled standards for relative quantification (15 µL per 50 µL CSF) were added to the peptide solutions followed by acidification to a final concentration of 0.1% TFA and 1% FA (pH ≤ 2). Sample plates were placed on an orbital shaker (300 rpm) for at least 10 minutes to ensure proper mixing. Plates were centrifuged (4680 rpm) for 30 minutes to pellet the precipitated surfactant. Peptides were desalted with Oasis PRiME HLB 96-well, 30mg sorbent per well, solid phase extraction (SPE) cleanup plates from Waters Corporation (Milford, MA) using a positive pressure system. Each SPE well was conditioned (500 µL methanol) and equilibrated twice (500 µL 0.1% TFA) before 500 µL 0.1% TFA and supernatant were added. Each well was washed twice (500 µL 0.1% TFA) and eluted twice (100 µL 50% acetonitrile/0.1% formic acid). All eluates were dried under centrifugal vacuum and reconstituted in 50 µL mobile phase A (0.1% FA in water) containing Promega 6 × 5 LC-MS/MS Peptide Reference Mix (50 fmol/µL; Promega V7491).

Liquid chromatography-tandem mass spectrometry (LC-MS/MS)

Peptides were analyzed using a TSQ Altis Triple Quadrupole mass spectrometer (Thermo Fisher Scientific). Each sample was injected (20 µL) using a 1290 Infinity II system (Agilent) and separated on an AdvanceBio Peptide Map Guard column (2.1x5mm, 2.7 µm, Agilent) connected to AdvanceBio Peptide Mapping analytical column (2.1x150mm, 2.7 µm, Agilent). Sample elution was performed over a 14-min gradient using mobile phase A (MPA; 0.1% FA in water) and mobile phase B (MPB; 0.1% FA in acetonitrile) with flow rate at 0.4 mL/min. The gradient was from 2% to 24% MPB over 12.1 minutes, then from 24% to 80% over 0.2 min and held at 80% B for 0.7 min. The mass spectrometer was set to acquire data in positive-ion mode using selected reaction monitoring (SRM) acquisition. Positive ion spray voltage was set to 3500 V for the Heated ESI source. The ion transfer tube and vaporizer temperatures were set to 325°C and 375°C, respectively. SRM transitions were acquired at Q1 resolution 0.7 FWHM, Q2 resolution 1.2 FWHM, CID gas 1.5 mTorr, 0.8 s cycle time.

Data analysis

Raw files from Altis TSQ were uploaded to Skyline-daily software (version 21.2.1.455), which was used for peak integration and quantification by peptide ratios. QC SRM data were manually evaluated in Skyline by assessing retention time reproducibility, matching light and heavy transitions using Ratio Dot Product, and determining the peptide ratio precision using CV by QC condition. If Skyline could not automatically pick a consistent peak due to interference in the light transitions the peptide was removed from the analysis. Transition profiles were checked to insure the heavy and light transition profiles matched using the Ratio

Dot Product value in Skyline. The Ratio Dot Product (1 = exact match) is a measure of whether the transition peak areas in the two label types are in the same ratio to each other. The average Ratio Dot Product value for each peptide was >0.90 for each QCs. If the retention time or Ratio Dot Product were outside of the expected range for a peptide in a few samples, the peaks were checked individually and adjusted as necessary. Total area ratios for each peptide were calculated in Skyline by summing the area for each light (3) and heavy (3) transition and dividing the light total area by the heavy total area. The Total Area Ratio CV was assessed using Skyline and the peptide was removed from the analysis if the CV>20% by QC condition. Next, the individual CSF samples were analyzed in a blinded fashion. We used the total area ratios (peptide ratios) for each targeted peptide in each sample and QC analysis; therefore, there are no missing values in the Data Matrix on Synapse. The raw data files and Skyline file have been deposited on Synapse[22].

Statistical analyses

We used Skyline-daily software (version 21.2.1.455) and GraphPad Prism (version 9.4.1) software to calculate means, medians, standard deviations, and coefficients of variations[24]. Peptide abundance ratios were log2-transformed, and zero values were imputed as one-half the minimum nonzero abundance measurement. Then, one-way ANOVA with Tukey *post hoc* tests for significance of the paired groupwise differences across diagnosis groups was performed in R (version 4.0.2) using a custom calculation and volcano plotting framework implemented and available as an open-source set of R functions documented further on https://www.github.com/edammer/parANOVA. T test p values and Benjamini-Hochberg FDR for these are reported for two total group comparisons, as was the case for AT+ versus AT- peptide mean difference significance calculations. Receiver-operating characteristic (ROC) analysis was performed in R (version 4.0.2) with a generalized linear model binomial fit of each set of peptide ratio measurements to the binary case diagnosis subsets AD/Control, AsymAD/Control, and AD/AsymAD using the pROC package implementing ROC curve plots, and calculations of AUC and AUC DeLong 95% confidence interval. Additional ROC curve characteristics including sensitivity, specificity, and accuracy were calculated with the reportROC R package. Robustness of the ROC calculations of AUC were confirmed using k-fold cross validation (k=10 folds, with each fold containing case subsets with equal distributions of the binary outcome) implemented using the cvAUC R package functions for calculating cross-validated AUC (cvAUC), and confidence interval on pooled predictions, and these calculations were consistently within 1 percent of AUC as calculated using a single calculation on the full data (data not shown). Venn diagrams were generated using the R vennEuler package, and the heatmap was produced using the R pheatmap package/function. R boxplot function output was overlaid with beeswarm-positioned individual measurement points using the R beeswarm package. Pearson correlations of SRM peptide measurements to immunoassay measurements of Aβ(1-42), total Tau, phospho-T181 Tau, and the ratio of total Tau/ Aβ were performed using the corAndPvalue WGCNA function in R. Correlation scatterplots were generated using the verboseScatterplot WGCNA function.

Data Records

All files have been deposited on Synapse[22]. The data folder contains sample traits, transition details, the peptide ratio data matrix, transition ratios, and protein details. The Metadata file contains the available traits for each sample analyzed including: SampleID – Internal Sample Identifier; Age(years) – Deidentified Age in years; Sex – Binary Sex; Race – self identified race; Educ – formal years of education; MoCA – Montreal Cognitive Assessment Score ranging from 0-30; APOE status – APOE genotype; Aβ42, tTau, pTau – as measured in CSF by Roche Elecsys® immunoassay platform; tTau:Aβ42 – ratio of tTau/ Aβ42; SampleRunOrder – the order the samples were acquired; Condition – the Control/AsymAD/AD group used in the analysis. The

DataMatrix file contains peptide ratio data for each sample. Data file names are list in the top row of the DataMatrix: AT+ QC samples begin with AD_; AT- QC samples begin with CTL_; Individual samples can be mapped back to the Metadata using the sample run order (Sxxx) or SampleID (_xxxxx); Plate/box and well position also defined in the file name (_Bx_Axx). The MS RAW files folder contains all mass spectrometry raw files (N=423) from both quality control replicates and clinical samples. The Skyline quantification folder contains the Skyline file that was used to report the peptide ratios, calculate CVs and means, and ratio dot product.

Technical Validation

Assessing peptide precision using pooled CSF quality control (QC) standards

We generated two pools of CSF reference standards as QCs based on biomarker status (AT- and AT+). These QCs were processed and analyzed (at the beginning, end, and after every 20 samples per plate) identically to the individual clinical samples for testing assay reproducibility. We analyzed 30 QCs (15 AT- and 15 AT+) over approximately 5 days during the run of clinical samples. We identified 62 peptides from 51 proteins as reliably measured in the pooled reference standards. Notably, only 5 of these peptides overlap with previous published PRM dataset given the unique differences in sample preparation, MS platform and peptide selection[21]. We included 58 peptides from 51 proteins in our biomarker analysis, plus peptides specific for the four APOE alleles for proteogenomic confirmation of APOE genotypes[27,28]. The technical coefficient of variation (CV) of each peptide was calculated based on the peptide area ratio for the biomarker negative (AT-) and positive (AT+) QCs. We defined CSF peptide biomarkers with CVs ≤ 20% as quantified with high precision in these technical replicates which were un-depleted and unfractionated CSF sample pools. Technical and process reproducibility for all reported peptides was below 20% (CV < 20%) in at least one pooled reference standard. The average CVs for all peptides in the AT- and AT+ QCs were 13% and 12%, respectively. **Supplemental Table 1** contains the QC statistics for the biomarker and APOE allele specific peptides. Levels of HBA and HBB peptides can be used to assess the levels of potential blood contamination[29] in each of the CSF samples across individual plates (**Supplemental Fig. 1**). Correction for blood contamination could improve the statistics; however, no correction was performed for the statistical analyses presented. We used the protein directions of change to assess accuracy in the QC pools. The volcano plot between peptides measured in the pools highlights peptide/protein levels that are consistent with previously reported AD biomarkers (**Supplemental Fig. 2**)[16,21].

Monitoring LC-MS/MS instrument performance

The sample reconstitution solution contained Promega 6×5 LC-MS/MS Peptide Reference Mix (50 fmol/µL)[30]. The Promega Peptide Reference Mix provides a convenient way to assess LC column performance and MS instrument parameters, including sensitivity and dynamic range. The mix consists of 30 peptides; 6 sets of 5 isotopologues of the same peptide sequence, differing only in the number of stable, heavy-labeled amino acids incorporated into the sequence using uniform 13C and 15N atoms making them chromatographically indistinguishable. The isotopologues were specifically synthesized to cover a wide range of hydrophobicities so that dynamic range could be assess across the gradient profile (**Fig. 2A**). Each isotopologue represents a series of 10-fold dilutions, estimated to be 1 pmole, 100 fmole, 10 fmole, 1 fmole, and 100 amole for each peptide sequence in a 20 µL injection, a range that would challenge the lowest limits of detection of the method (**Fig. 2B**). We assessed the raw peak areas in 423 injections over 5 days to determine the label-free CV for each peptide isotopologue (**Fig. 2B**). The 100-amole level (0.0001x) was not detected (ND) for any of the peptide sequences. Based on the label-free CV, we determined the lowest limit of detection for each peptide to be between 1-10 fmole across the gradient profile with a dynamic range

spanning 4 orders of magnitude for all peptides except the latest eluting peptide at 13.3 minutes (**Fig. 2C**).

Technical replicate variance

Three individual samples were analyzed in duplicate scattered throughout the sample run sequence to assess technical replicate variance. We graphed the log2(ratio) for each of 58 biomarker peptides in replicate 1 versus replicate 2 for each sample and determined the Pearson correlation coefficient with associated P value (**Supplemental Fig. 3**). The analysis showed a near-identical correlation (ρ=0.996-0.998; p<1e-200) between each of the technical replicate pairs for the three individual CSF samples, supporting the same high level of method reproducibility we found using the QC pools.

Concordance between a discovery (ssTMT) and replication (SRM) datasets

Since our peptide targets were largely based on multiple ssTMT datasets[16], we generated a representative ssTMT peptide level volcano from one of these datasets comprised of 297 individuals (147 control and 150 AD) (**Fig. 3A**). There are 44 of 62 SRM peptides that overlap with this ssTMT dataset and are highlighted in yellow on the volcano plot (**Fig. 3A**). To establish peptide concordance, we also compared the direction of change or effect size (log2 fold change) for 40 overlapping peptides, excluding albumin, hemoglobin, and APOE allele specific peptides. **Fig. 3B** shows significant correlation (cor = 0.91; p = 2.8e-15) between SRM and ssTMT peptide highlighting the accuracy and concordance of measurements across both MS assays. Thus, despite substantial differences in chromatography (nanoflow versus standard flow), MS instrumentation (Orbitrap versus triple quadrupole), and protein quantitation approaches (ssTMT versus SRM), the selected peptides in this assay are highly reproducible and robust in their direction of change in AD CSF.

Usage Notes

This targeted mass spectrometry dataset serves as a valuable resource for a variety of research endeavors including, but not limited to, the following applications:

Use case 1: Peptide abundance in CSF

This dataset provides a reference for peptide detectability in CSF under relatively high-throughput conditions, especially if an investigator wants to determine whether their protein of interest has abundance above the lower limit of detection in CSF under these analytical conditions. Raw data deposited on Synapse[22] contains transitions for over 200 peptides that were robustly detected in CSF discovery proteomics[16,21].

Use case 2: Using APOE allele specific peptides for genotyping

Apolipoprotein E (ApoE) has three major genetic variants (E2, E3, and E4, encoded by the ε2, ε3 and ε4 alleles, respectively) that differ by single amino acid substitutions[31]. APOE genotype is closely related to AD risk[32] with ApoE4 having the highest risk, ApoE2 the lowest risk, and ApoE3 with intermediate risk[33,34]. Due to the amino acid substitutions in each variant, there are allele specific peptides that can be targeted by mass spectrometry[27,35]. We monitored CLAVYQAGAR (APOE2), LGADMEDVR (APOE4), LGADMEDVCGR (APOE2 or APOE3), and LAVYQAGAR (APOE3 or APOE4) to confirm the APOE genotype of each CSF sample in a concurrent SRM-MS method[22]. The CV for each APOE peptide in each QC is listed in **Supplemental Table 1**. Previous studies report the association of APOE genotype with various clinical, neuroimaging, and biomarker measures[36-39]. Exploring the relationship between APOE status and the CSF biomarker peptides presented requires further analysis reserved for future studies.

Use case 3: Stage-specific differences in peptide and protein levels

361 The described cohort includes control, AsymAD, and AD groups across the
362 Amyloid/Tau/Neurodegeneration (AT/N) framework[40], which allows for the comparison of
363 peptide and protein differential abundance across stages of disease. Investigators can focus
364 on comparisons that are specific to symptomatic AD or those with potential for staging AD by
365 using the AsymAD group compared to the control group. By comparing candidate biomarkers
366 using ANOVA (excluding APOE allele specific peptides), we found 41 differentially expressed
367 peptides (36 proteins) in AsymAD vs controls (**Fig. 4A**), 35 differentially expressed peptides (30
368 proteins) in AD versus controls (**Fig. 4B**), and 21 differentially expressed peptides (18 proteins)
369 in AD vs AsymAD (**Fig. 4C**). The Venn diagram summarizes the differentially expressed peptides
370 across groups in **Fig. 4D**.

371 Using a differential abundance analysis, we were able to stratify the changing proteins as early
372 or progressive biomarkers of AD (**Fig. 4 and 5**). The $\log_2$-fold change (Log_2 FC) from the volcano
373 plots in **Fig. 4** are represented as a heatmap in **Fig. 5A** to illustrate how each peptide is
374 changing across each group comparison. Twenty-two peptides (21 proteins) were early
375 biomarkers of AD because they were significantly different in AsymAD versus controls, but not
376 significantly different in AD versus AsymAD (**Fig. 5A**). A plurality of these proteins mapped to
377 metabolic enzymes linked to glucose metabolism (PKM, MDH1, ENO1, ALDOA, ENO2, LDHB,
378 and TPI1, also in **Supplemental Table 2**)[13,14]. SMOC1 and SPP1, markers linked to glial biology
379 and inflammation[14,16], were also increased in AsymAD samples compared to controls (**Fig. 5B**,
380 *top row*). GAPDH, YWHAB and YWHAZ proteins were found to be progressive biomarkers of
381 AD because the proteins were differentially expressed from Control to AsymAD and from
382 AsymAD to AD with a consistent trend in direction of change (**Fig. 5B**, *middle row*). Proteins
383 associated with neuronal/synaptic markers including VGF, NPTX2, NPTXR, and L1CAM were
384 increased in AsymAD compared to controls but decreased in AD vs controls (**Fig. 5B**, *lower*
385 *row*). Interestingly, we found 14 peptides (13 proteins) that were up in AsymAD as compared
386 to Control but down in AD when compared to AsymAD. A majority of these proteins map to
387 neuronal/synaptic markers including VGF, NPTX2, NPTXR, which are some of the most
388 correlated proteins in post-mortem brain to an individual's slope of cognitive trajectory in life
389 (**Fig. 5A and 5B,** *lower row*)[41].

390 **Use case 4: Correlation of peptide biomarker abundance to Aβ(1-42), Tau, pTau and**
391 **cognitive measures**

392 The comparison of existing biomarkers to the SRM peptide measurements can be
393 accomplished by correlation, where the degree of correlation indicates how similar a peptide
394 measurement is to the established immunoassay-measured biomarkers of Aβ(1-42), total Tau,
395 and pTau as well as cognition (MoCA score). In **Fig. 6A**, we demonstrate that 57 of the 58
396 biomarker peptides have significant correlation to at least one of the above biomarkers, or the
397 ratio of total Tau/Aβ. Individual correlation scatterplots and linear fit lines for three of the
398 peptides (SMOC1: AQALEQAK, YWHAZ: VVSSIEQK, and VGF: EPVAGDAVPGPK) are provided in
399 **Fig. 6B**. Significant correlations of these peptides to the established biomarker and cognitive
400 measures indicate the potential of these measurements to classify or stage disease
401 progression. The targeted SRM measurement correlations largely agree with those observed
402 from unbiased discovery proteomics[42] and parallel reaction monitoring[21] experiments.

403 **Use case 5: Receiver-operating characteristic (ROC) analysis for evaluating biomarker**
404 **diagnostic capability**

405 The capacity for peptide measurements to serve as a diagnostic biomarker distinguishing
406 individuals with AD and even asymptomatic disease from individuals not on a trajectory to
407 develop AD is well-established, with secreted amyloid and tau peptide measurements in CSF
408 being the current gold standard for interrogation of patients' AD stage from their CSF[43] where
409 CSF Aβ(1-42) concentration inversely correlates to plaque deposition in the living brain[44]. The
410 measurements of additional peptides collected here are appropriate for comparison to

immunoassay measurements of CSF amyloid and Tau biomarker positivity, or a dichotomized cognition rating, or other ancillary traits such as diagnosis for the 390 individuals. To demonstrate this utility, we performed receiver-operating characteristic (ROC) curve analysis and calculated the area under the curve (AUC) for all 62 peptide measures as fitting a logistic regression to 3 subsets of samples divided to represent known pairs of disease stages, namely AD versus control, AsymAD versus control, and AD vs AsymAD (**Fig. 7** and **Supplemental Table 4**). The top performing peptide for the YWHAZ gene product 14-3-3 ζ protein demonstrated an AUC of 89.5% discrimination of AD from control cases consistent with previous studies[21,45,46]. SMOC1 AUC of 81.8% was the best performing peptide for discrimination of AsymAD from control groups. In contrast, the synaptic peptides to NPTX2 (AUC of 74.0%), NPTXR (AUC of 71.1%), VGF (AUC of 70.1%) and SCG2 (AUC of 69.8%) best discriminated AD from AsymAD groups suggesting that neurodegeneration due to AD pathology is occurring in the symptomatic phase of disease[47]. **Fig. 7** shows the top five peptides by AUC for each of the three comparisons, highlighting the potential of this data set to aid in the design or validation of stage-specific biomarkers. Additional future analysis using these peptides alone or in combination could be used to subtype, predict disease onset, and gauge treatment efficacy.

Code Availability

Custom code generating use case figures and tables including correlation plots, volcanoes, Venn diagram, annotated heatmap, statistics tables, and ROC curves is available for download with registration for a free account on synapse.org. The code is available as R scripts from https://doi.org/10.7303/syn35927166 (the Analysis folder) deposited on Synapse[22]. These scripts were run as provided on R version 4.0.2 with the two provided input files to generate outputs.

Acknowledgements

This study was supported by the following National Institutes of Health funding mechanisms: U01AG061357 (A.I.L and N.T.S), R01AG070937-01 (J.J.L) and P30AG066511 (A.I.L). We acknowledge our colleagues at Emory for providing critical feedback.

Author contributions

Conceptualization, C.M.W., L.P., D.M.D., J.J.L., A.I.L., B.R.R, N.T.S.; Methodology, C.M.W., E.B.D, L.P., D.M.D., E.M., E.K.C., B.R.R, N.T.S.; Investigation and Formal Analysis, C.M.W., E.B.D, L.P., D.M.D., B.R.R, N.T.S.; Writing – Original Draft, C.M.W., E.B.D., N.T.S.; Writing – Review and Editing, C.M.W., E.C.B.J, B.R.R., J.J.L., A.I.L., N.T.S.; Funding Acquisition, A.I.L. and N.T.S.; Supervision, N.T.S.

Competing interests

The authors declare no competing interests.

Figure Legends

Figure 1. Cohort characteristics. A total of 390 samples (133 controls, 127 AsymAD, 130 AD unless otherwise noted) were analyzed using the following characteristics for grouping. (**A**) Age range across each group of the cohort was carefully selected to balance for age and sex (**Supplemental Table 1**). (**B**) Cognition was assessed using the Montreal Cognitive Assessment (MoCA) score; there is no significant difference in scores between the Control and AsymAD groups serving as the two cognitively normal diagnostic groups (133 controls, 127 AsymAD, 124 AD). The Roche Diagnostics Elecsys® platform was used for CSF biomarker measurements for Aβ(1-42) (**C**), Total Tau (133 controls, 127 AsymAD, 129 AD) (**D**), and pTau (**E**) (pg/mL) showing the significance between groups for each measurement. (**F**) Tau/Aβ ratio data across

control, AsymAD and AD groups. There was no significant difference between AsymAD and AD groups to serve as our biomarker positive groups (133 controls, 127 AsymAD, 129 AD). The significance of the pairwise comparisons is indicated by overlain annotation of 'ns' (not significant; $p>0.05$) or asterisks; ****$p\leq0.0001$.

Figure 2. Isotopologue peptide internal reference standards to determine consistency of LC-MS/MS platform. Each of the CSF samples were spiked with a six-peptide, 5 isotopologue concentration LC-MS/MS Peptide Reference Mix from Promega (50 fmol/µL). (**A**) Extracted ion chromatogram for the 6 peptide (1pmol) mixture illustrating the wide range of retention times due to their hydrophobicity. (**B**) The raw peak areas in 423 injections over 5 days were used to determine the label-free CV for each peptide isotopologue estimating the lowest limits of detection to be between 1-10 fmole for each peptide. (**C**) The 5 unique isotopologues are used to assess the dynamic range across the gradient profile and each peptide demonstrates linearity across 3-4 orders of magnitude in the batch of 423 injections. Error bars represent the standard deviation across 423 injections.

Figure 3. Peptide concordance between SRM and ssTMT datasets. (**A**) Volcano plot displaying the $\log_2$ fold change (FC) (x-axis) against t-test log10 p-value (y-axis) for all peptides (n=2,340) comparing AD (n=150) versus Controls (n=147). Cutoffs were determined by significant differential expression ($p<0.05$) between control and AD cases. Peptides with significantly decreased levels in AD are shown in blue while peptides with significantly increased levels in disease were indicated in red. 44 of 62 SRM peptides that overlap with this ssTMT dataset and SRM are highlighted as larger yellow points with black text labels. Red text and traces to red points are labels for peptides not included in the current SRM study that were significantly upregulated in the ssTMT dataset. (**B**) Correlation between the fold-change (AD vs control) of all selected overlapping peptides (n=40) across SRM (x-axis) and ssTMT (y-axis) were strongly correlated (cor=0.91, $p=2.8e-15$).

Figure 4. Differential expression analysis across stages of AD. ANOVA analysis with Tukey *post hoc* FDR was performed for pairwise comparison of mean $\log_2$(ratio) differences between the 3 stages of AD (i.e., Control, AsymAD and AD) of N=390 total case samples and plotted as a volcano. Significance threshold for counting of peptides was $p < 0.05$ (dashed horizontal line). Differentially expressed peptides for (**A**) AsymAD (N=127) versus control (N=133), (**B**) AD (N=130) versus control, and (**C**) AD versus AsymAD are labeled by their gene symbols. (**D**) Counts of peptides with significant difference in any of the 3 dichotomous comparisons are presented as a Venn diagram. Full statistics from the ANOVA and Tukey post-hoc analysis is presented in **Supplemental Table 2**.

Figure 5. Stratifying early from progressive biomarkers of AD. (**A**) The magnitude of positive (red) and negative (blue) changes are shown on a gradient color scale heatmap representing mean $\log_2$-fold change (Log_2FC) for each of 49 peptides significant in any of the 3 group comparisons. Tukey significance of the pairwise comparisons is indicated by overlain asterisks; *$p<0.05$, **$p<0.01$, ***$p<0.001$. (**B**) Peptide abundance levels of selected panel markers that are differentially expressed between groups. The upper row highlights biomarkers that are significantly different in AsymAD versus controls, but not significantly different in AsymAD versus AD. The middle row of 3 peptides highlights progressive biomarkers of AD, which show a stepwise increase in abundance from control to AsymAD to AD cases. The bottom row highlights a set of proteins that are increased in AsymAD compared to controls but decreased in AD versus control or AsymAD samples.

Figure 6. Correlating CSF peptide biomarker abundances to amyloid, Tau, and cognitive measures. (**A**) Positive (red) and negative (blue) Pearson correlations between biomarker peptide abundance and immunoassay measures of Aβ(1-42), total Tau, phospho-T181 Tau (pTau), ratio of total Tau/Aβ and cognition (MoCA score). Student's *t* test significance is indicated by overlain asterisks; *p<0.05, **p<0.01, ***p<0.001. (**B**) Individual correlation scatterplots are shown for SMOC1 (upper row), YWHAZ (middle row), and VGF (lower row). Individual cases are colored by their diagnosis; blue for controls, red for AsymAD cases, and green for AD cases. Amyloid immunoassay measures of 1,700 (maximum, saturated value in the assay) were not considered for correlation.

Figure 7. Receiver-operating characteristic (ROC) curve analysis of peptide diagnostic potential. ROC curves for each of three pairs of diagnosed case groups were generated to determine the top-ranked diagnostic biomarker peptides among the 58-peptide panel plus 4 APOE specific peptides. (**A**) A total of 263 AD (N=130) and control (N=133) CSF case samples were classified according to the logistic fit for each peptide's $\log_2$(ratio) measurements across these samples, and the top 5 ranked by AUC are shown. (**B**) Top five performing peptides for discerning AsymAD (N=127) from control (N=133) case diagnosis groups are provided with AUCs, nominating these peptides as potential markers of pre-symptomatic disease, and as cognates for AT+ biomarker positivity. (**C**) Symptomatic AD (N=130) and AsymAD (N=127) discerning peptides were ranked by AUC and the top five ROC curves are shown and nominated as cognate CSF measures for compromised patient cognition.

Supplemental Data

Supplemental Figure 1. Monitoring background peptide levels in CSF. Three proteins were monitored for levels of potential blood contamination in each of the CSF samples. The peptide ratio for hemoglobin subunit alpha (**A**), hemoglobin subunit beta (**B**), and albumin (**C** and **D**) peptides are plotted for each of the CSF samples (N=423) in acquisition order.

Supplemental Figure 2. Differentially abundant peptides representing changed proteins in AT- vs AT+ QC CSF pools. The differentially abundant proteins in the QC pools were used to check the accuracy of the fold change consistent with our other studies[16]. We found 21 upregulated and 10 downregulated peptides. This result validated the direction of change of six proteins nominally significantly downregulated in previously published discovery proteomics (PON1, APOC1, NPTX2, VGF, NPTXR, and SCG2), and of sixteen proteins previously reported as upregulated (YWHAZ, GDA, CHI3L1, PKM, CALM2, SMOC1, YWHAB, MDH1, ALDOA, ENO1, GOT1, PPIA, DDAH1, PEBP1, PARK7, and SPP1)[16,21].

Supplemental Figure 3. Technical reproducibility of peptide measurements in replicate CSF samples. Pearson correlation and p-value of replicate measures of 58 peptides in the 3 replicated CSF samples that were analyzed randomly within the series of 423 injections by SRM-MS.

Supplemental Table 1. Coefficient of variation (CV) values for 58 biomarker peptides and APOE allele specific peptides in AT- and AT+ QC pools.

Supplemental Table 2. ANOVA of differential abundance analysis for 58 biomarker peptides across Control, AsymAD and AD sample pairwise group comparisons. The SRM proteins were also cross-referenced with protein data and module membership from Johnson et al. Consensus Network[48], and mapped to CSF protein panels from Higginbotham et al. Integrated Proteomic analysis[16].

Supplemental Table 3. Pearson correlations (rho), Student p values of correlation significance, and numbers of paired observations for correlation of biomarker peptide abundances to immunoassay measures of Aβ(1-42), total Tau, phospho-T181 Tau, and the ratio of total Tau/ Aβ.

Supplemental Table 4. ROC curve statistics including AUC, p, 95% DeLong confidence interval, accuracy, specificity, and sensitivity for dichotomous diagnosis case sample groups.

References

1 Scheltens, P. *et al.* Alzheimer's disease. *The Lancet* **397**, 1577-1590, doi:10.1016/S0140-6736(20)32205-4 (2021).

2 Duyckaerts, C., Delatour, B. & Potier, M.-C. Classification and basic pathology of Alzheimer disease. *Acta neuropathologica* **118**, 5-36 (2009).

3 Jack Jr, C. R. *et al.* NIA-AA research framework: toward a biological definition of Alzheimer's disease. *Alzheimer's & Dementia* **14**, 535-562 (2018).

4 Mattsson-Carlgren, N. *et al.* Cerebrospinal fluid biomarkers in autopsy-confirmed Alzheimer disease and frontotemporal lobar degeneration. *Neurology* **98**, e1137-e1150 (2022).

5 Zetterberg, H. & Blennow, K. Moving fluid biomarkers for Alzheimer's disease from research tools to routine clinical diagnostics. *Molecular neurodegeneration* **16**, 1-7 (2021).

6 Long, J. M. & Holtzman, D. M. Alzheimer disease: an update on pathobiology and treatment strategies. *Cell* **179**, 312-339 (2019).

7 Rayaprolu, S. *et al.* Systems-based proteomics to resolve the biology of Alzheimer's disease beyond amyloid and tau. *Neuropsychopharmacology* **46**, 98-115 (2021).

8 Sperling, R. A. *et al.* Toward defining the preclinical stages of Alzheimer's disease: Recommendations from the National Institute on Aging-Alzheimer's Association workgroups on diagnostic guidelines for Alzheimer's disease. *Alzheimer's & dementia* **7**, 280-292 (2011).

9 Dubois, B. *et al.* Preclinical Alzheimer's disease: definition, natural history, and diagnostic criteria. *Alzheimer's & Dementia* **12**, 292-323 (2016).

10 Hasin, Y., Seldin, M. & Lusis, A. Multi-omics approaches to disease. *Genome biology* **18**, 1-15 (2017).

11 Seyfried, N. T. *et al.* A Multi-network Approach Identifies Protein-Specific Co-expression in Asymptomatic and Symptomatic Alzheimer's Disease. *Cell Syst* **4**, 60-72 e64, doi:10.1016/j.cels.2016.11.006 (2017).

12 Johnson, E. C. B. *et al.* Deep proteomic network analysis of Alzheimer's disease brain reveals alterations in RNA binding proteins and RNA splicing associated with disease. *Mol Neurodegener* **13**, 52, doi:10.1186/s13024-018-0282-4 (2018).

13 Johnson, E. C. B. *et al.* A Consensus Proteomic Analysis of Alzheimer's Disease Brain and Cerebrospinal Fluid Reveals Early Changes in Energy Metabolism Associated with Microglia and Astrocyte Activation. *bioRxiv*, 802959, doi:10.1101/802959 (2019).

14 Johnson, E. C. *et al.* Large-scale proteomic analysis of Alzheimer's disease brain and cerebrospinal fluid reveals early changes in energy metabolism associated with microglia and astrocyte activation. *Nature medicine* **26**, 769-780 (2020).

15 Blennow, K. & Zetterberg, H. Biomarkers for Alzheimer's disease: current status and prospects for the future. *Journal of internal medicine* **284**, 643-663 (2018).

16 Higginbotham, L. *et al.* Integrated proteomics reveals brain-based cerebrospinal fluid biomarkers in asymptomatic and symptomatic Alzheimer's disease. *Science advances* **6**, eaaz9360 (2020).

613 17 Picotti, P. & Aebersold, R. Selected reaction monitoring–based proteomics: workflows,
614 potential, pitfalls and future directions. *Nature methods* **9**, 555-566 (2012).
615 18 Bittner, T. *et al.* Technical performance of a novel, fully automated
616 electrochemiluminescence immunoassay for the quantitation of beta-amyloid (1-42)
617 in human cerebrospinal fluid. *Alzheimers Dement* **12**, 517-526,
618 doi:10.1016/j.jalz.2015.09.009 (2016).
619 19 Hansson, O. *et al.* CSF biomarkers of Alzheimer's disease concord with amyloid-beta
620 PET and predict clinical progression: A study of fully automated immunoassays in
621 BioFINDER and ADNI cohorts. *Alzheimers Dement* **14**, 1470-1481,
622 doi:10.1016/j.jalz.2018.01.010 (2018).
623 20 Schindler, S. E. *et al.* Cerebrospinal fluid biomarkers measured by Elecsys assays
624 compared to amyloid imaging. *Alzheimers Dement*, doi:10.1016/j.jalz.2018.01.013
625 (2018).
626 21 Zhou, M. *et al.* Targeted mass spectrometry to quantify brain-derived cerebrospinal
627 fluid biomarkers in Alzheimer's disease. *Clinical Proteomics* **17**, 1-14 (2020).
628 22 Watson, C. M., Dammer, E.B., and Seyfried, N.T. Emory AD CSF SRM. *Synapse*,
629 doi:https://doi.org/10.7303/syn34054965 (2022).
630 23 MacLean, B. *et al.* Skyline: an open source document editor for creating and analyzing
631 targeted proteomics experiments. *Bioinformatics* **26**, 966-968 (2010).
632 24 Pino, L. K. *et al.* The Skyline ecosystem: Informatics for quantitative mass spectrometry
633 proteomics. *Mass spectrometry reviews* **39**, 229-244 (2020).
634 25 MacLean, B. *et al.* Effect of collision energy optimization on the measurement of
635 peptides by selected reaction monitoring (SRM) mass spectrometry. *Analytical*
636 *chemistry* **82**, 10116-10124 (2010).
637 26 Kulak, N. A., Pichler, G., Paron, I., Nagaraj, N. & Mann, M. Minimal, encapsulated
638 proteomic-sample processing applied to copy-number estimation in eukaryotic cells.
639 *Nature methods* **11**, 319-324 (2014).
640 27 Simon, R. *et al.* Total ApoE and ApoE4 isoform assays in an Alzheimer's disease case-
641 control study by targeted mass spectrometry (n= 669): a pilot assay for methionine-
642 containing proteotypic peptides. *Molecular & Cellular Proteomics* **11**, 1389-1403
643 (2012).
644 28 Rezeli, M. *et al.* Quantification of total apolipoprotein E and its specific isoforms in
645 cerebrospinal fluid and blood in Alzheimer's disease and other neurodegenerative
646 diseases. *EuPA Open Proteomics* **8**, 137-143 (2015).
647 29 Geyer, P. E. *et al.* Plasma Proteome Profiling to detect and avoid sample-related biases
648 in biomarker studies. *EMBO molecular medicine* **11**, e10427 (2019).
649 30 Beri, J., Rosenblatt, M. M., Strauss, E., Urh, M. & Bereman, M. S. Reagent for evaluating
650 liquid chromatography–tandem mass spectrometry (LC-MS/MS) performance in
651 bottom-up proteomic experiments. *Analytical chemistry* **87**, 11635-11640 (2015).
652 31 Hatters, D. M., Peters-Libeu, C. A. & Weisgraber, K. H. Apolipoprotein E structure:
653 insights into function. *Trends in biochemical sciences* **31**, 445-454 (2006).
654 32 Saunders, A. M. *et al.* Association of apolipoprotein E allele ϵ4 with late-onset familial
655 and sporadic Alzheimer's disease. *Neurology* **43**, 1467-1467 (1993).
656 33 Farrer, L. A. *et al.* Effects of age, sex, and ethnicity on the association between
657 apolipoprotein E genotype and Alzheimer disease. A meta-analysis. APOE and
658 Alzheimer Disease Meta Analysis Consortium. *JAMA* **278**, 1349-1356 (1997).
659 34 Heffernan, A. L., Chidgey, C., Peng, P., Masters, C. L. & Roberts, B. R. The neurobiology
660 and age-related prevalence of the ε4 allele of apolipoprotein E in Alzheimer's disease
661 cohorts. *Journal of Molecular Neuroscience* **60**, 316-324 (2016).
662 35 Minta, K. *et al.* Quantification of total apolipoprotein E and its isoforms in
663 cerebrospinal fluid from patients with neurodegenerative diseases. *Alzheimer's*
664 *research & therapy* **12**, 1-11 (2020).

36 Bussy, A. *et al.* Effect of apolipoprotein E4 on clinical, neuroimaging, and biomarker measures in noncarrier participants in the Dominantly Inherited Alzheimer Network. *Neurobiology of aging* **75**, 42-50 (2019).

37 El-Lebedy, D., Raslan, H. M. & Mohammed, A. M. Apolipoprotein E gene polymorphism and risk of type 2 diabetes and cardiovascular disease. *Cardiovascular diabetology* **15**, 1-11 (2016).

38 Morris, J. C. *et al.* APOE predicts amyloid-beta but not tau Alzheimer pathology in cognitively normal aging. *Ann Neurol* **67**, 122-131, doi:10.1002/ana.21843 (2010).

39 Grimmer, T. *et al.* Progression of cerebral amyloid load is associated with the apolipoprotein E ε4 genotype in Alzheimer's disease. *Biological psychiatry* **68**, 879-884 (2010).

40 Knopman, D. S. *et al.* The National Institute on Aging and the Alzheimer's Association research framework for Alzheimer's disease: perspectives from the research roundtable. *Alzheimer's & Dementia* **14**, 563-575 (2018).

41 Wingo, A. P. *et al.* Large-scale proteomic analysis of human brain identifies proteins associated with cognitive trajectory in advanced age. *Nature communications* **10**, 1-14 (2019).

42 Dammer, E. B. *et al.* Multi-Platform Proteomic Analysis of Alzheimer's Disease Cerebrospinal Fluid and Plasma Reveals Network Biomarkers Associated with Proteostasis and the Matrisome. *bioRxiv* (2022).

43 Bertens, D., Knol, D. L., Scheltens, P. & Visser, P. J. Temporal evolution of biomarkers and cognitive markers in the asymptomatic, MCI, and dementia stage of Alzheimer's disease. *Alzheimer's & Dementia* **11**, 511-522, doi:https://doi.org/10.1016/j.jalz.2014.05.1754 (2015).

44 Shokouhi, S. *et al.* Reference tissue normalization in longitudinal 18F-florbetapir positron emission tomography of late mild cognitive impairment. *Alzheimer's Research & Therapy* **8**, 2, doi:10.1186/s13195-016-0172-3 (2016).

45 Sathe, G. *et al.* Quantitative proteomic profiling of cerebrospinal fluid to identify candidate biomarkers for Alzheimer's disease. *PROTEOMICS–Clinical Applications* **13**, 1800105 (2019).

46 Bader, J. M. *et al.* Proteome profiling in cerebrospinal fluid reveals novel biomarkers of Alzheimer's disease. *Molecular systems biology* **16**, e9356 (2020).

47 Libiger, O. *et al.* Longitudinal CSF proteomics identifies NPTX2 as a prognostic biomarker of Alzheimer's disease. *Alzheimer's & Dementia* **17**, 1976-1987 (2021).

48 Johnson, E. C. *et al.* Large-scale deep multi-layer analysis of Alzheimer’s disease brain reveals strong proteomic disease-related changes not observed at the RNA level. *Nature neuroscience* **25**, 213-225 (2022).

Table 1. Cohort Characteristics

Sample Group	CT	AsymAD	AD
Sample Size	N=133	N=127	N=130
Characteristics			
Sex	99 F, 34 M	94 F, 33 M	97 F, 33 M
Age [a]	66 ± 6	66 ± 6	66 ± 6
MoCA [b]	26.8 ± 2.0	26.4 ± 2.6	17.4 ± 5.5
$A\beta_{42}$ [b]	1394.0 ± 280.7	752.0 ± 238.2	587.0 ± 236.8
tTau [b]	165.8 ± 35.0	260.8 ± 97.2	375.7 ± 139.6
pTau [b]	14.7 ± 3.2	25.2 ± 11.1	38.5 ± 15.5

[a] Age in years. Values given as average ± standard deviation

[b] MoCA, $A\beta_{42}$, tTau, and pTau in pg/mL. Values given in average ± standard deviation

Abbreviations: CT, Control; AD, Alzheimer's disease; MoCA, Montreal Cognitive Assessment

Figure 1

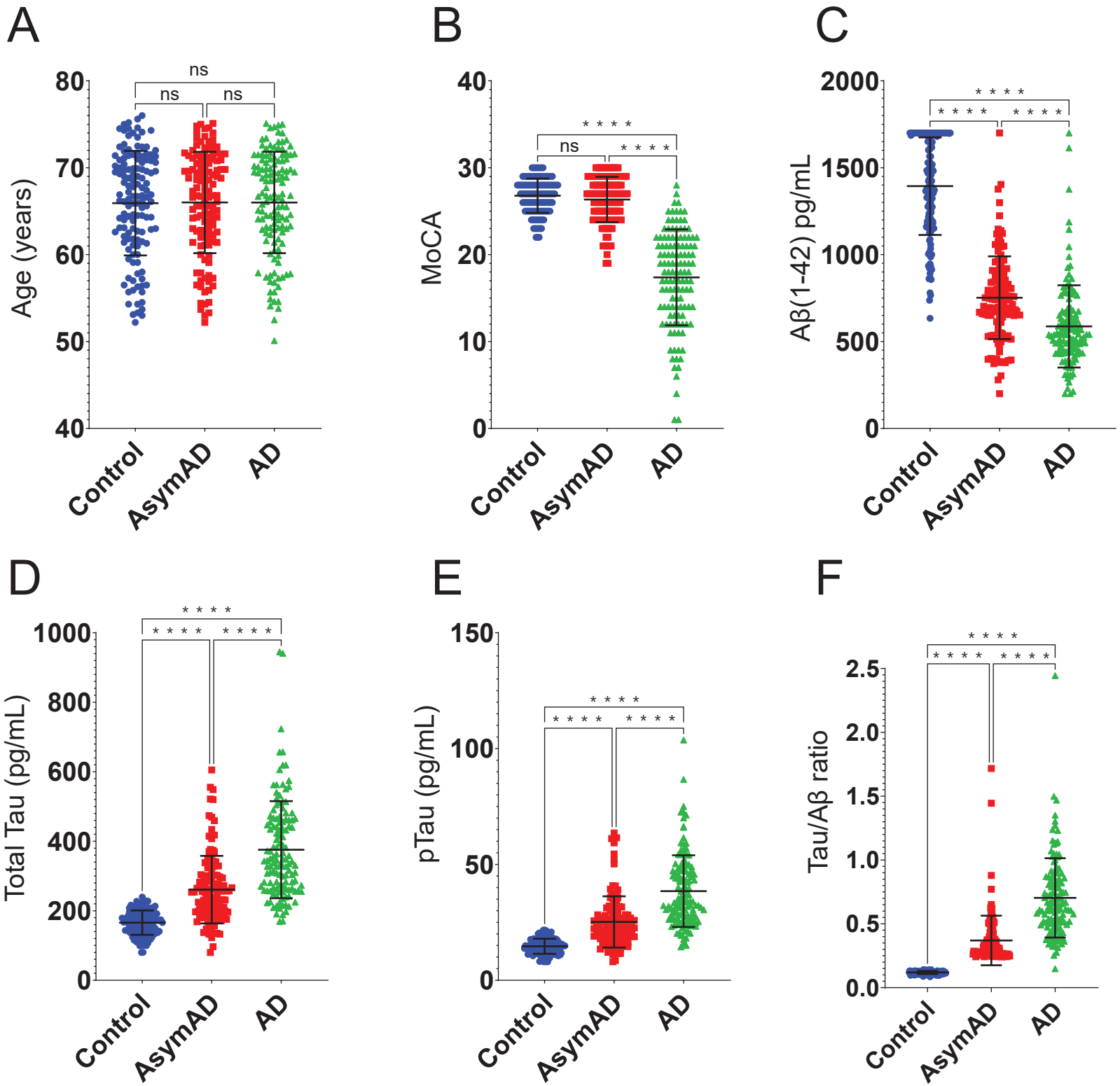
A
Age (years)
80
70
60
50
40
ns
ns
ns
Control
AsymAD
AD
B
MoCA
40
30
20
10
0
* * * *
ns
* * * *
Control
AsymAD
AD
C
Aβ(1-42) pg/mL
2000
1500
1000
500
0
* * * *
* * * *
* * * *
Control
AsymAD
AD
D
Total Tau (pg/mL)
1000
800
600
400
200
0
* * * *
* * * *
* * * *
Control
AsymAD
AD
E
pTau (pg/mL)
150
100
50
0
* * * *
* * * *
* * * *
Control
AsymAD
AD
F
Tau/Aβ ratio
2.5
2.0
1.5
1.0
0.5
0.0
* * * *
* * * *
* * * *
Control
AsymAD
AD

Figure 2

A

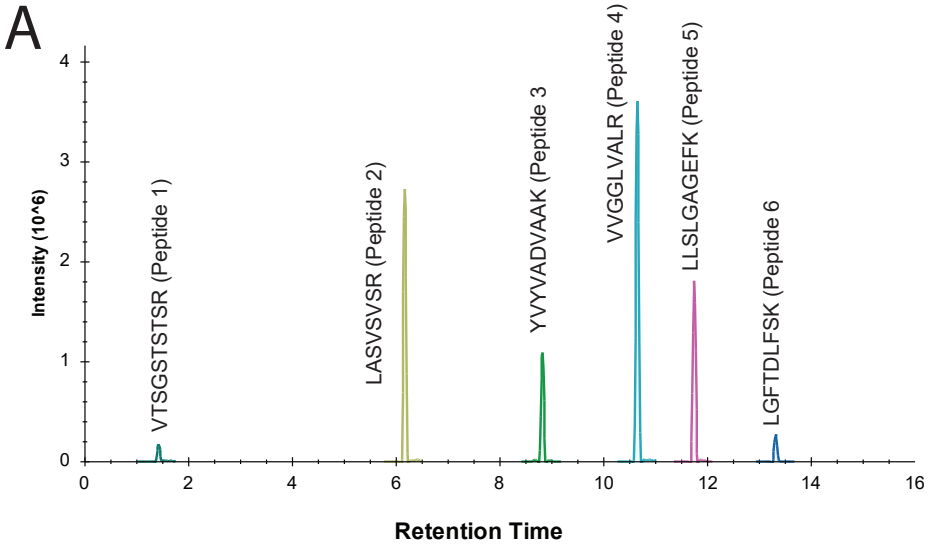

B

Promega Peptide Sequence	Average Retention Time (min)	1 pmole (1x)	100 fmole (0.1x)	10 fmole (0.01x)	1 fmole (0.001x)	100 amole (0.0001x)
VTSGSTSTSR	1.42	17%	17%	18%	34%	ND
LASVSVSR	6.17	7%	8%	8%	17%	ND
YVYVADVAAK	8.83	11%	11%	13%	32%	ND
VVGGLVALR	10.65	8%	8%	9%	20%	ND
LLSLGAGEFK	11.75	9%	9%	10%	20%	ND
LGFTDLFSK	13.33	21%	21%	30%	ND	ND

C

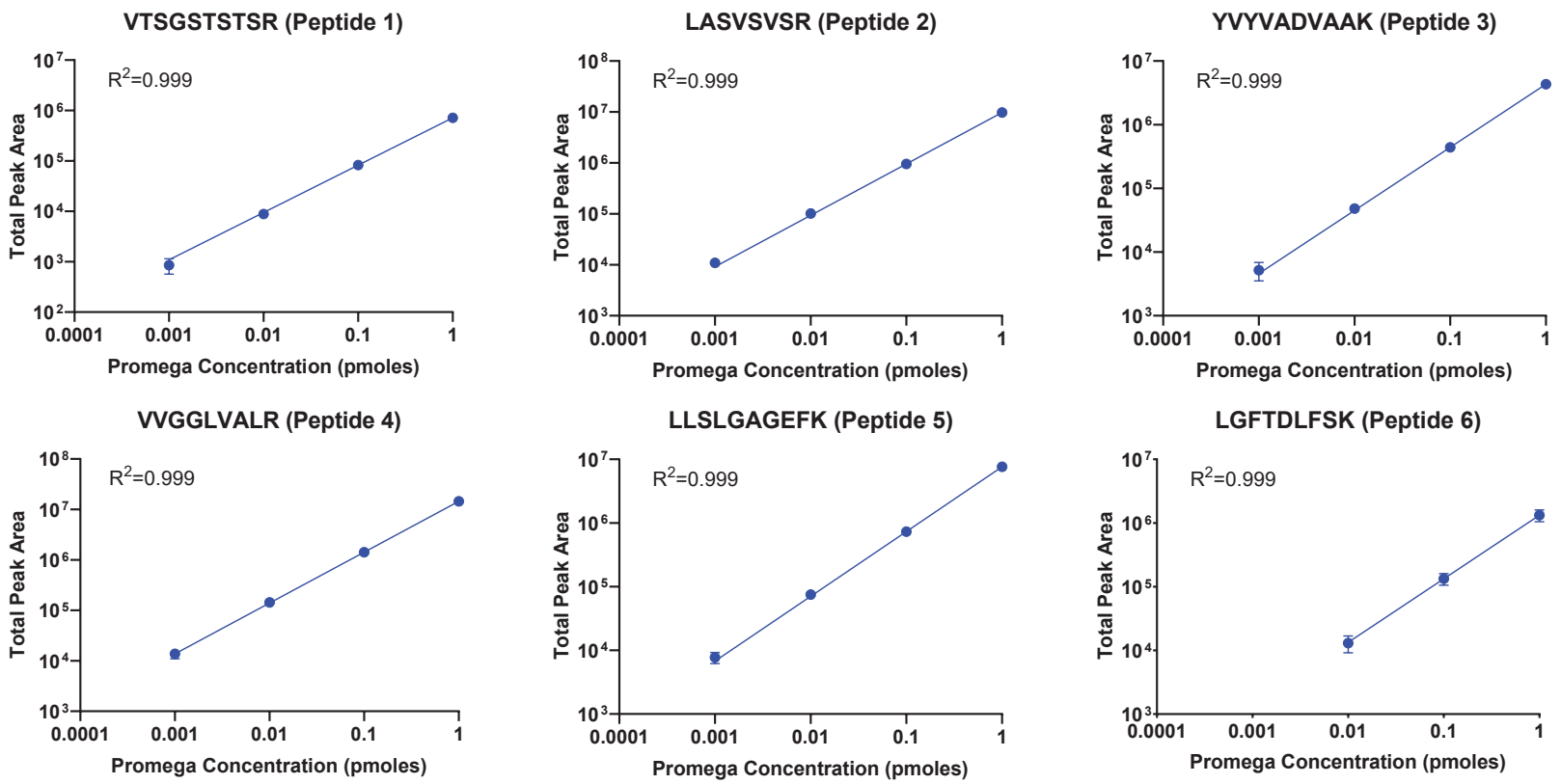

Figure 3

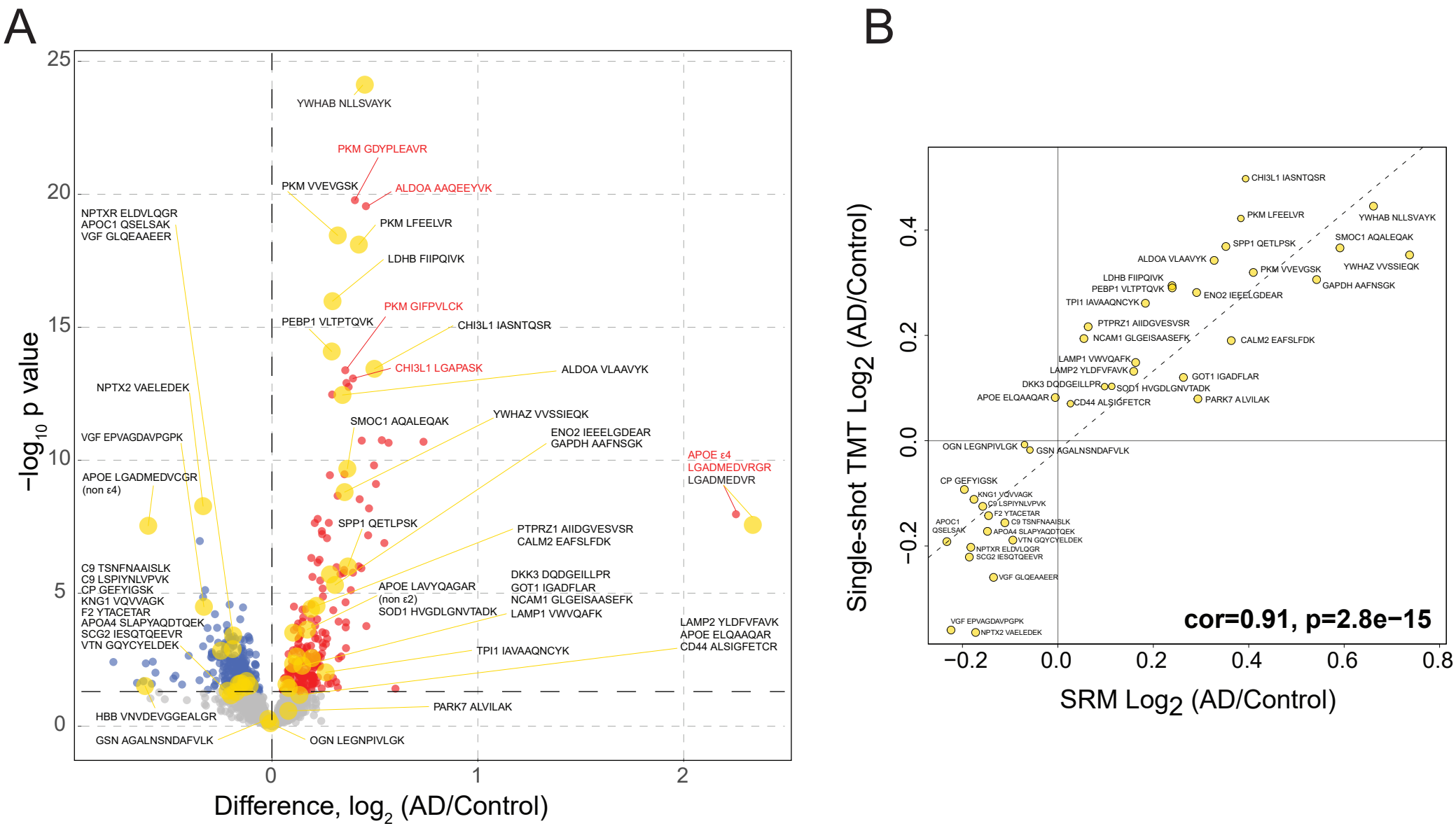
A
B
−log10 p value
Difference, log2 (AD/Control)
YWHAB NLLSVAYK
PKM GDYPLEAVR
PKM VVEVGSK
ALDOA AAQEEYVK
NPTXR ELDVLQGR
APOC1 QSELSAK
VGF GLQEAAEER
PKM LFEELVR
LDHB FIIPQIVK
PKM GIFPVLCK
PEBP1 VLTPTQVK
CHI3L1 IASNTQSR
CHI3L1 LGAPASK
ALDOA VLAAVYK
NPTX2 VAELEDEK
SMOC1 AQALEQAK
YWHAZ VVSSIEQK
ENO2 IEEELGDEAR
GAPDH AAFNSGK
VGF EPVAGDAVPGPK
APOE ε4
LGADMEDVRGR
LGADMEDVR
APOE LGADMEDVCGR
(non ε4)
SPP1 QETLPSK
PTPRZ1 AIIDGVESVSR
CALM2 EAFSLFDK
C9 TSNFNAAISLK
C9 LSPIYNLVPVK
CP GEFYIGSK
KNG1 VQVVAGK
F2 YTACETAR
APOA4 SLAPYAQDTQEK
SCG2 IESQTQEEVR
VTN GQYCYELDEK
APOE LAVYQAGAR
(non ε2)
SOD1 HVGDLGNVTADK
DKK3 DQDGEILLPR
GOT1 IGADFLAR
NCAM1 GLGEISAASEFK
LAMP1 VWVQAFK
LAMP2 YLDFVFAVK
APOE ELQAAQAR
CD44 ALSIGFETCR
TPI1 IAVAAQNCYK
PARK7 ALVILAK
HBB VNVDEVGGEALGR
GSN AGALNSNDAFVLK
OGN LEGNPIVLGK
Single-shot TMT Log2 (AD/Control)
SRM Log2 (AD/Control)
cor=0.91, p=2.8e−15

Figure 4

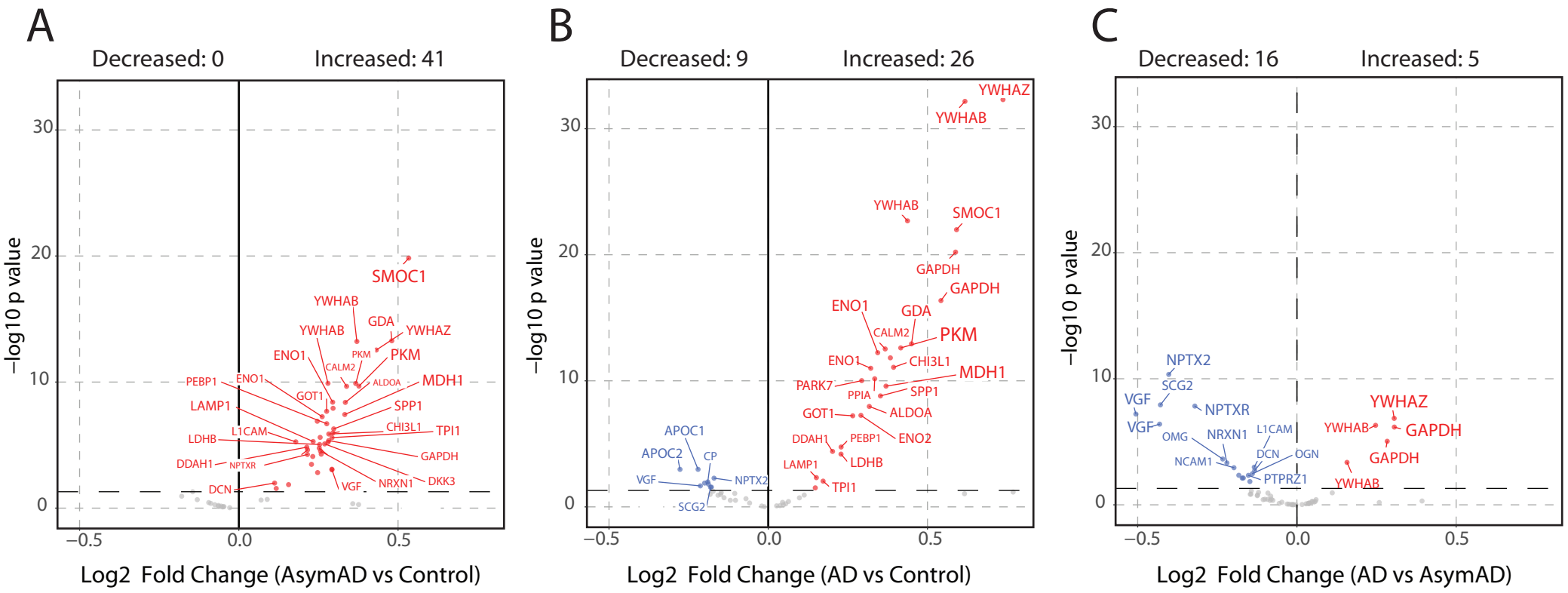
A
Decreased: 0
Increased: 41
−log10 p value
Log2 Fold Change (AsymAD vs Control)
SMOC1
YWHAB
GDA
YWHAZ
PKM
ENO1
CALM2
ALDOA
MDH1
PEBP1
GOT1
SPP1
LAMP1
CHI3L1
TPI1
L1CAM
LDHB
GAPDH
DDAH1
NPTXR
NRXN1
DKK3
DCN
VGF
B
Decreased: 9
Increased: 26
Log2 Fold Change (AD vs Control)
YWHAZ
YWHAB
SMOC1
GAPDH
ENO1
GDA
CALM2
PKM
CHI3L1
MDH1
PARK7
PPIA
SPP1
ALDOA
GOT1
DDAH1
PEBP1
ENO2
LDHB
LAMP1
TPI1
APOC1
APOC2
CP
VGF
NPTX2
SCG2
C
Decreased: 16
Increased: 5
Log2 Fold Change (AD vs AsymAD)
NPTX2
SCG2
VGF
NPTXR
YWHAZ
VGF
OMG
NRXN1
L1CAM
YWHAB
GAPDH
NCAM1
DCN
OGN
GAPDH
PTPRZ1
YWHAB
D
Differentially Abundant Peptides
AD vs Control
(35)
AD vs AsymAD
(21)
AsymAD vs Control
(41)
1
21
8
11
2
6

Figure 5

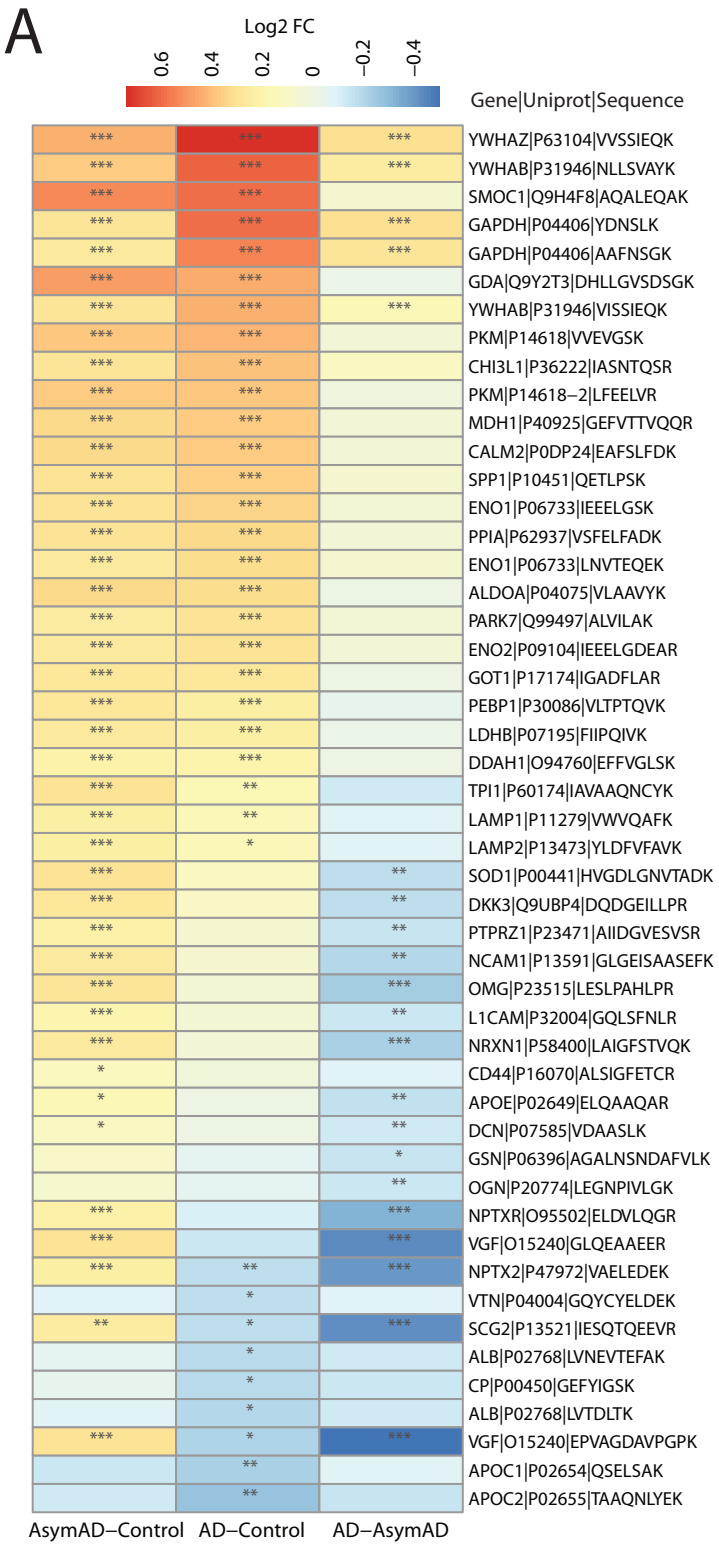
A
Log2 FC
0.6
0.4
0.2
0
−0.2
−0.4
Gene|Uniprot|Sequence
YWHAZ|P63104|VVSSIEQK
YWHAB|P31946|NLLSVAYK
SMOC1|Q9H4F8|AQALEQAK
GAPDH|P04406|YDNSLK
GAPDH|P04406|AAFNSGK
GDA|Q9Y2T3|DHLLGVSDSGK
YWHAB|P31946|VISSIEQK
PKM|P14618|VVEVGSK
CHI3L1|P36222|IASNTQSR
PKM|P14618−2|LFEELVR
MDH1|P40925|GEFVTTVQQR
CALM2|P0DP24|EAFSLFDK
SPP1|P10451|QETLPSK
ENO1|P06733|IEEELGSK
PPIA|P62937|VSFELFADK
ENO1|P06733|LNVTEQEK
ALDOA|P04075|VLAAVYK
PARK7|Q99497|ALVILAK
ENO2|P09104|IEEELGDEAR
GOT1|P17174|IGADFLAR
PEBP1|P30086|VLTPTQVK
LDHB|P07195|FIIPQIVK
DDAH1|O94760|EFFVGLSK
TPI1|P60174|IAVAAQNCYK
LAMP1|P11279|VWVQAFK
LAMP2|P13473|YLDFVFAVK
SOD1|P00441|HVGDLGNVTADK
DKK3|Q9UBP4|DQDGEILLPR
PTPRZ1|P23471|AIIDGVESVSR
NCAM1|P13591|GLGEISAASEFK
OMG|P23515|LESLPAHLPR
L1CAM|P32004|GQLSFNLR
NRXN1|P58400|LAIGFSTVQK
CD44|P16070|ALSIGFETCR
APOE|P02649|ELQAAQAR
DCN|P07585|VDAASLK
GSN|P06396|AGALNSNDAFVLK
OGN|P20774|LEGNPIVLGK
NPTXR|O95502|ELDVLQGR
VGF|O15240|GLQEAAEER
NPTX2|P47972|VAELEDEK
VTN|P04004|GQYCYELDEK
SCG2|P13521|IESQTQEEVR
ALB|P02768|LVNEVTEFAK
CP|P00450|GEFYIGSK
ALB|P02768|LVTDLTK
VGF|O15240|EPVAGDAVPGPK
APOC1|P02654|QSELSAK
APOC2|P02655|TAAQNLYEK
AsymAD−Control
AD−Control
AD−AsymAD

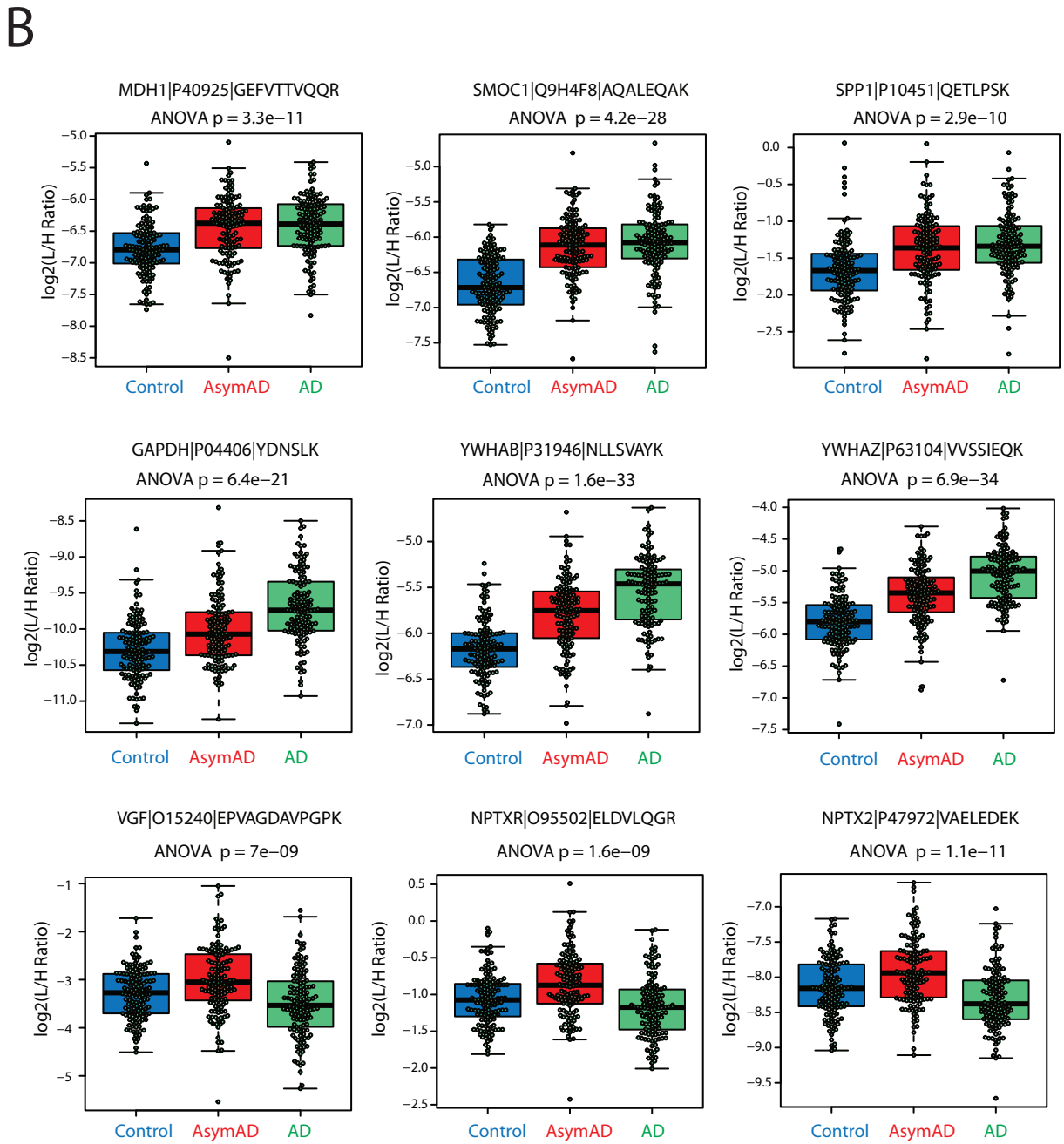
B
MDH1|P40925|GEFVTTVQQR
ANOVA p = 3.3e−11
SMOC1|Q9H4F8|AQALEQAK
ANOVA p = 4.2e−28
SPP1|P10451|QETLPSK
ANOVA p = 2.9e−10
GAPDH|P04406|YDNSLK
ANOVA p = 6.4e−21
YWHAB|P31946|NLLSVAYK
ANOVA p = 1.6e−33
YWHAZ|P63104|VVSSIEQK
ANOVA p = 6.9e−34
VGF|O15240|EPVAGDAVPGPK
ANOVA p = 7e−09
NPTXR|O95502|ELDVLQGR
ANOVA p = 1.6e−09
NPTX2|P47972|VAELEDEK
ANOVA p = 1.1e−11
log2(L/H Ratio)
Control
AsymAD
AD

Figure 6

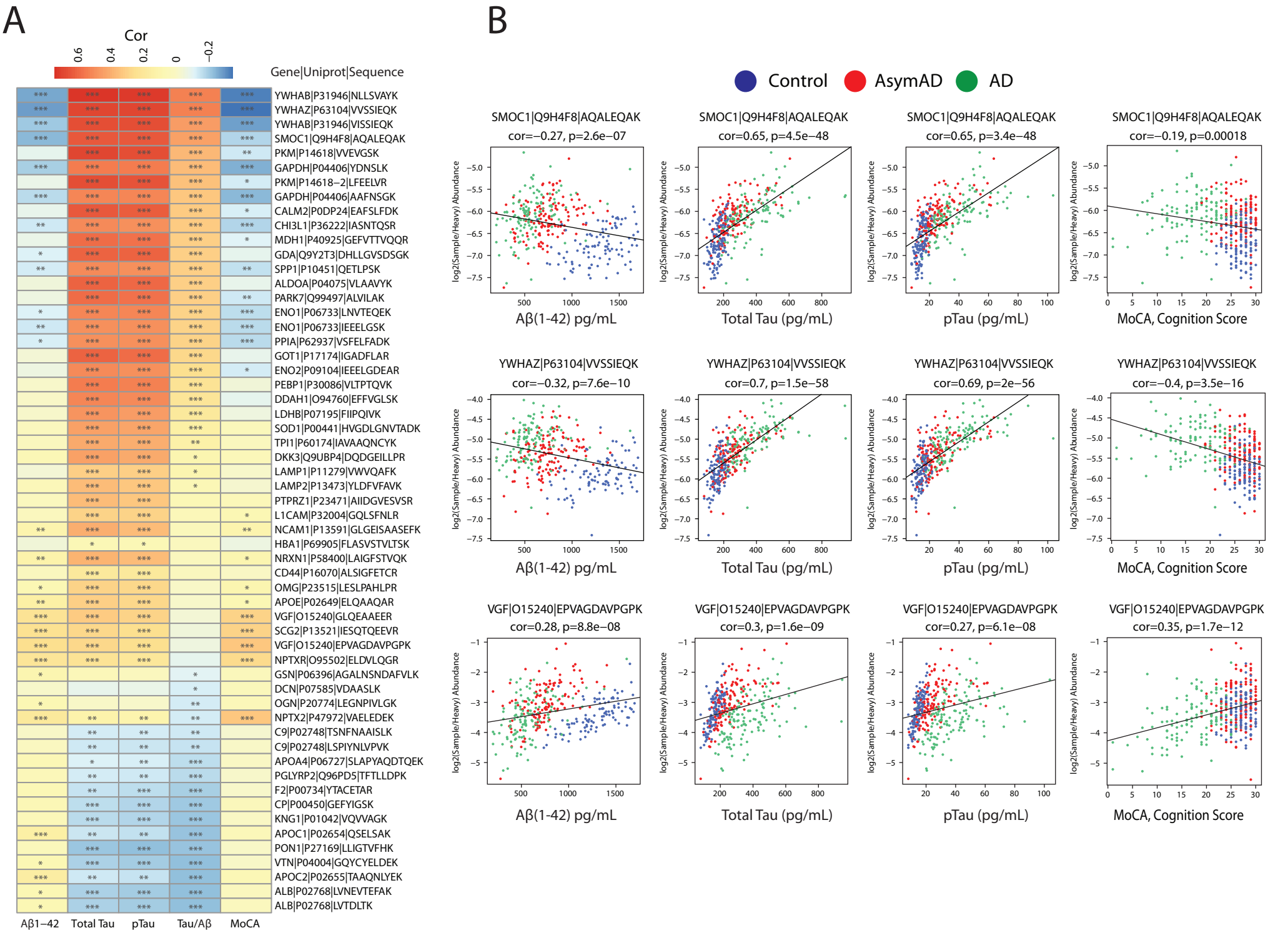
A
Cor
0.6
0.4
0.2
0
−0.2
Gene|Uniprot|Sequence
YWHAB|P31946|NLLSVAYK
YWHAZ|P63104|VVSSIEQK
YWHAB|P31946|VISSIEQK
SMOC1|Q9H4F8|AQALEQAK
PKM|P14618|VVEVGSK
GAPDH|P04406|YDNSLK
PKM|P14618−2|LFEELVR
GAPDH|P04406|AAFNSGK
CALM2|P0DP24|EAFSLFDK
CHI3L1|P36222|IASNTQSR
MDH1|P40925|GEFVTTVQQR
GDA|Q9Y2T3|DHLLGVSDSGK
SPP1|P10451|QETLPSK
ALDOA|P04075|VLAAVYK
PARK7|Q99497|ALVILAK
ENO1|P06733|LNVTEQEK
ENO1|P06733|IEEELGSK
PPIA|P62937|VSFELFADK
GOT1|P17174|IGADFLAR
ENO2|P09104|IEEELGDEAR
PEBP1|P30086|VLTPTQVK
DDAH1|O94760|EFFVGLSK
LDHB|P07195|FIIPQIVK
SOD1|P00441|HVGDLGNVTADK
TPI1|P60174|IAVAAQNCYK
DKK3|Q9UBP4|DQDGEILLPR
LAMP1|P11279|VWVQAFK
LAMP2|P13473|YLDFVFAVK
PTPRZ1|P23471|AIIDGVESVSR
L1CAM|P32004|GQLSFNLR
NCAM1|P13591|GLGEISAASEFK
HBA1|P69905|FLASVSTVLTSK
NRXN1|P58400|LAIGFSTVQK
CD44|P16070|ALSIGFETCR
OMG|P23515|LESLPAHLPR
APOE|P02649|ELQAAQAR
VGF|O15240|GLQEAAEER
SCG2|P13521|IESQTQEEVR
VGF|O15240|EPVAGDAVPGPK
NPTXR|O95502|ELDVLQGR
GSN|P06396|AGALNSNDAFVLK
DCN|P07585|VDAASLK
OGN|P20774|LEGNPIVLGK
NPTX2|P47972|VAELEDEK
C9|P02748|TSNFNAAISLK
C9|P02748|LSPIYNLVPVK
APOA4|P06727|SLAPYAQDTQEK
PGLYRP2|Q96PD5|TFTLLDPK
F2|P00734|YTACETAR
CP|P00450|GEFYIGSK
KNG1|P01042|VQVVAGK
APOC1|P02654|QSELSAK
PON1|P27169|LLIGTVFHK
VTN|P04004|GQYCYELDEK
APOC2|P02655|TAAQNLYEK
ALB|P02768|LVNEVTEFAK
ALB|P02768|LVTDLTK
Aβ1−42
Total Tau
pTau
Tau/Aβ
MoCA
B
Control
AsymAD
AD
SMOC1|Q9H4F8|AQALEQAK
cor=−0.27, p=2.6e−07
cor=0.65, p=4.5e−48
cor=0.65, p=3.4e−48
cor=−0.19, p=0.00018
YWHAZ|P63104|VVSSIEQK
cor=−0.32, p=7.6e−10
cor=0.7, p=1.5e−58
cor=0.69, p=2e−56
cor=−0.4, p=3.5e−16
VGF|O15240|EPVAGDAVPGPK
cor=0.28, p=8.8e−08
cor=0.3, p=1.6e−09
cor=0.27, p=6.1e−08
cor=0.35, p=1.7e−12
log2(Sample/Heavy) Abundance
Aβ(1-42) pg/mL
Total Tau (pg/mL)
pTau (pg/mL)
MoCA, Cognition Score

Figure 7

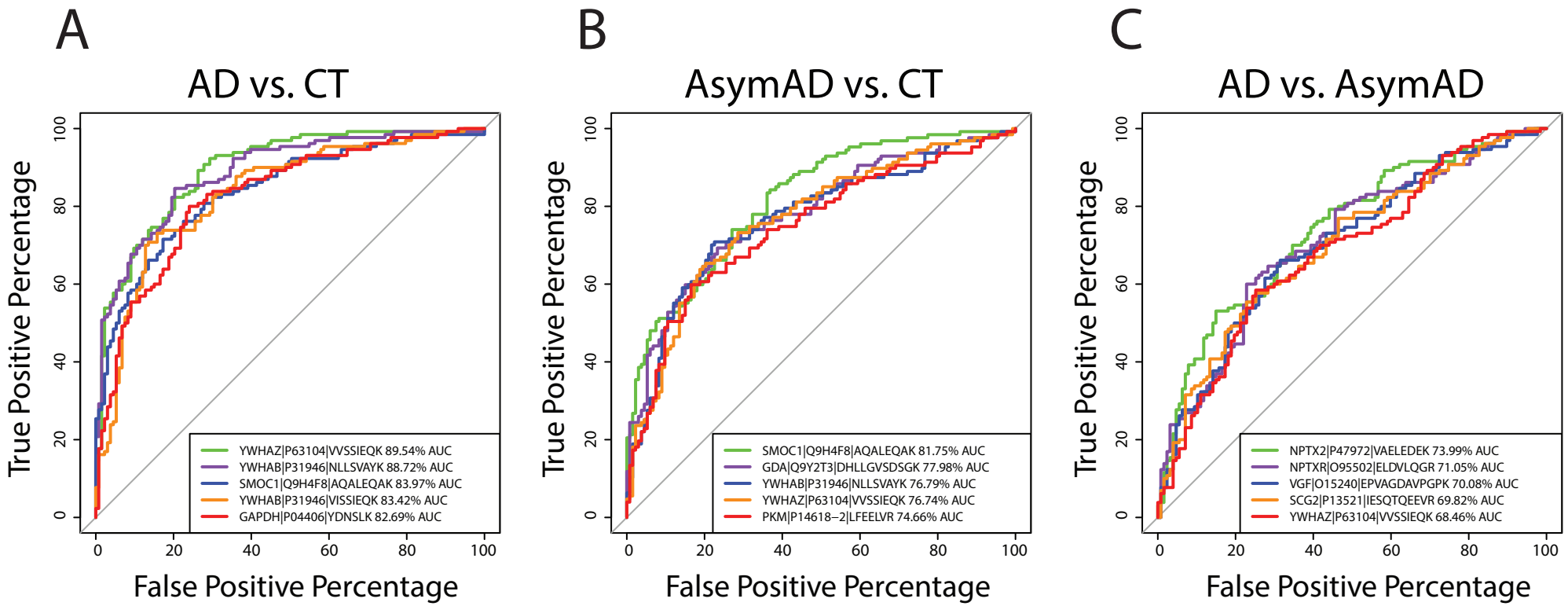
A
AD vs. CT
True Positive Percentage
False Positive Percentage
0
20
40
60
80
100
YWHAZ|P63104|VVSSIEQK 89.54% AUC
YWHAB|P31946|NLLSVAYK 88.72% AUC
SMOC1|Q9H4F8|AQALEQAK 83.97% AUC
YWHAB|P31946|VISSIEQK 83.42% AUC
GAPDH|P04406|YDNSLK 82.69% AUC
B
AsymAD vs. CT
True Positive Percentage
False Positive Percentage
SMOC1|Q9H4F8|AQALEQAK 81.75% AUC
GDA|Q9Y2T3|DHLLGVSDSGK 77.98% AUC
YWHAB|P31946|NLLSVAYK 76.79% AUC
YWHAZ|P63104|VVSSIEQK 76.74% AUC
PKM|P14618−2|LFEELVR 74.66% AUC
C
AD vs. AsymAD
True Positive Percentage
False Positive Percentage
NPTX2|P47972|VAELEDEK 73.99% AUC
NPTXR|O95502|ELDVLQGR 71.05% AUC
VGF|O15240|EPVAGDAVPGPK 70.08% AUC
SCG2|P13521|IESQTQEEVR 69.82% AUC
YWHAZ|P63104|VVSSIEQK 68.46% AUC

Supplemental Figure 1

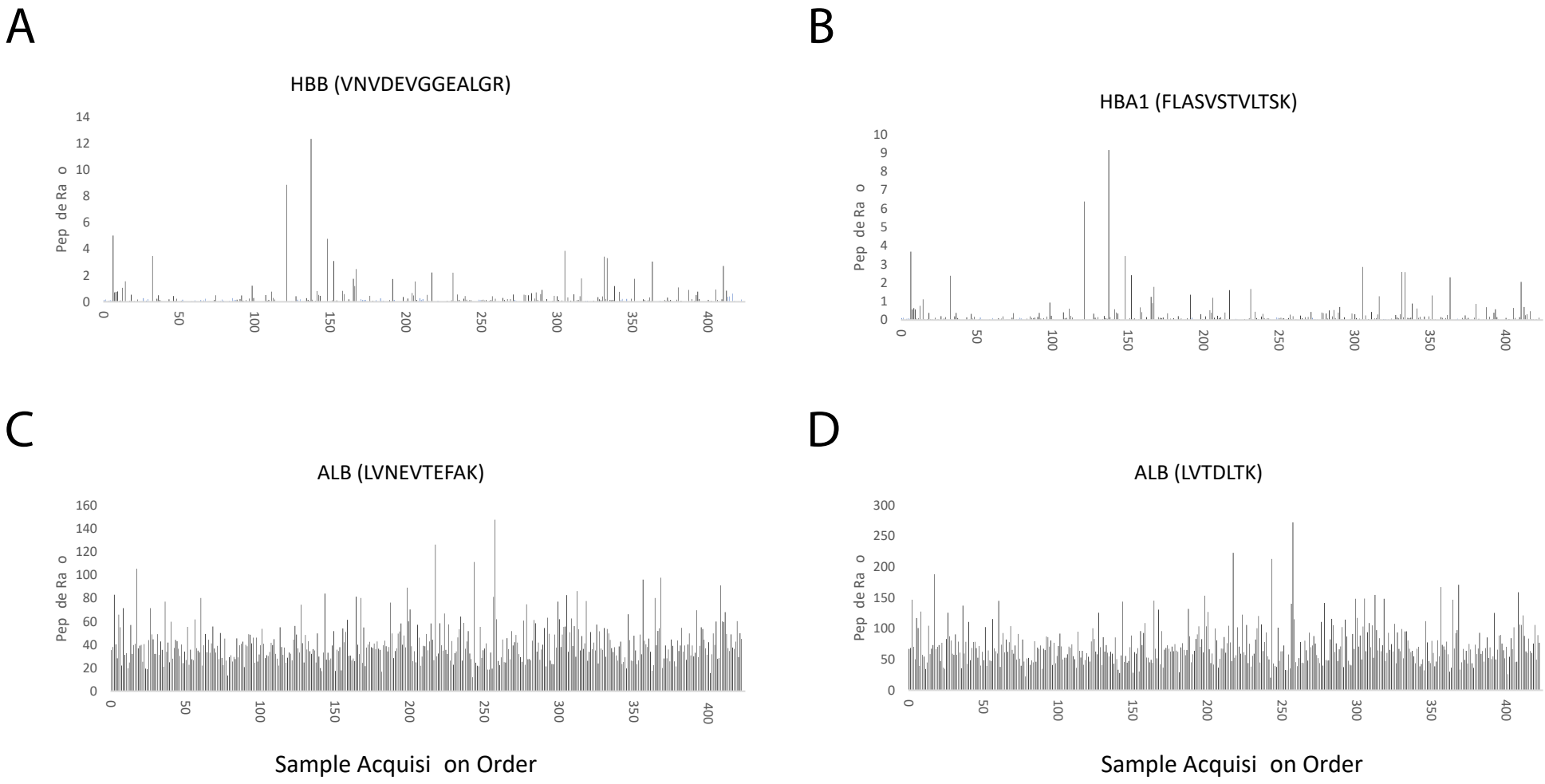

Supplemental Figure 2

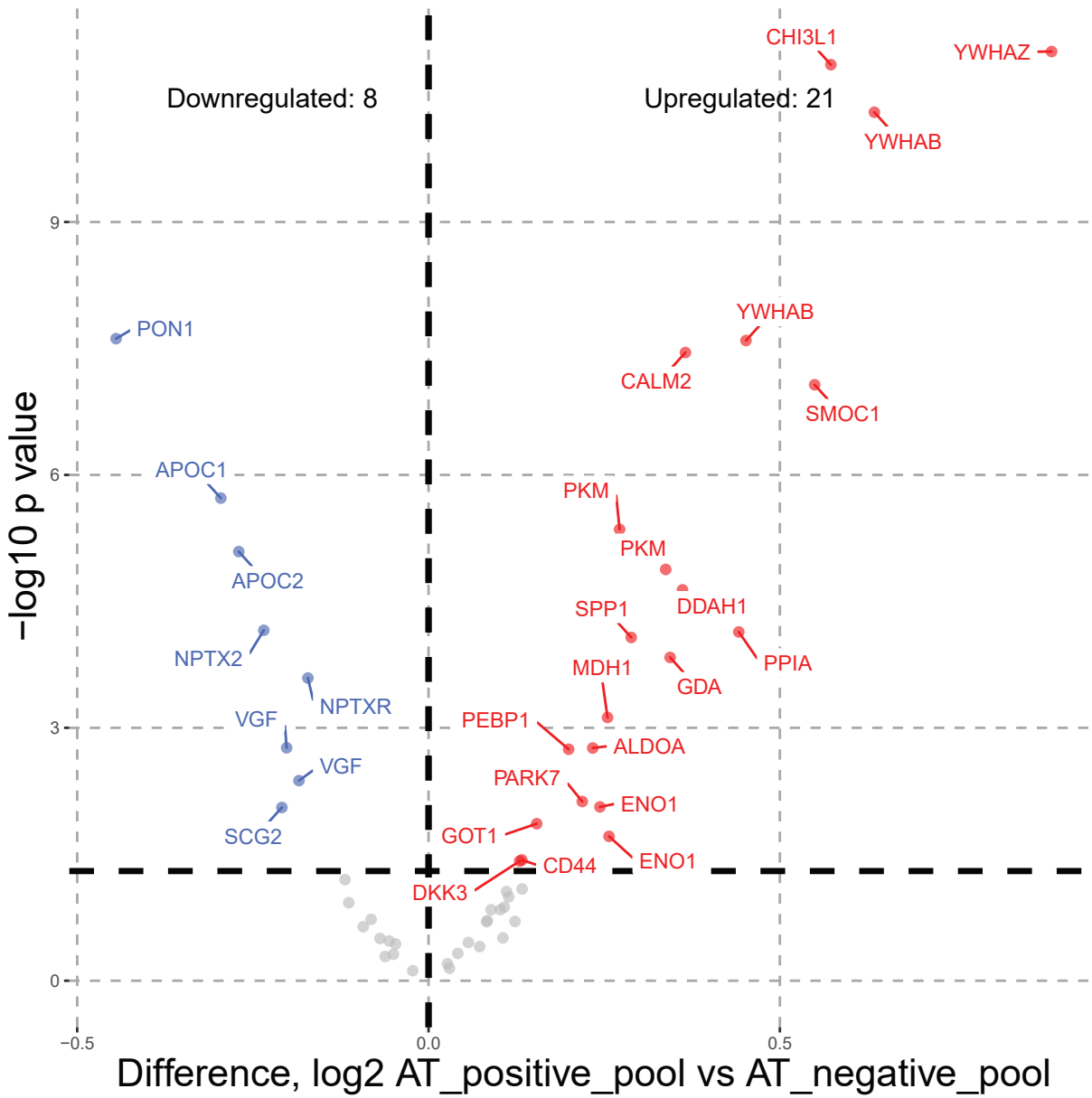
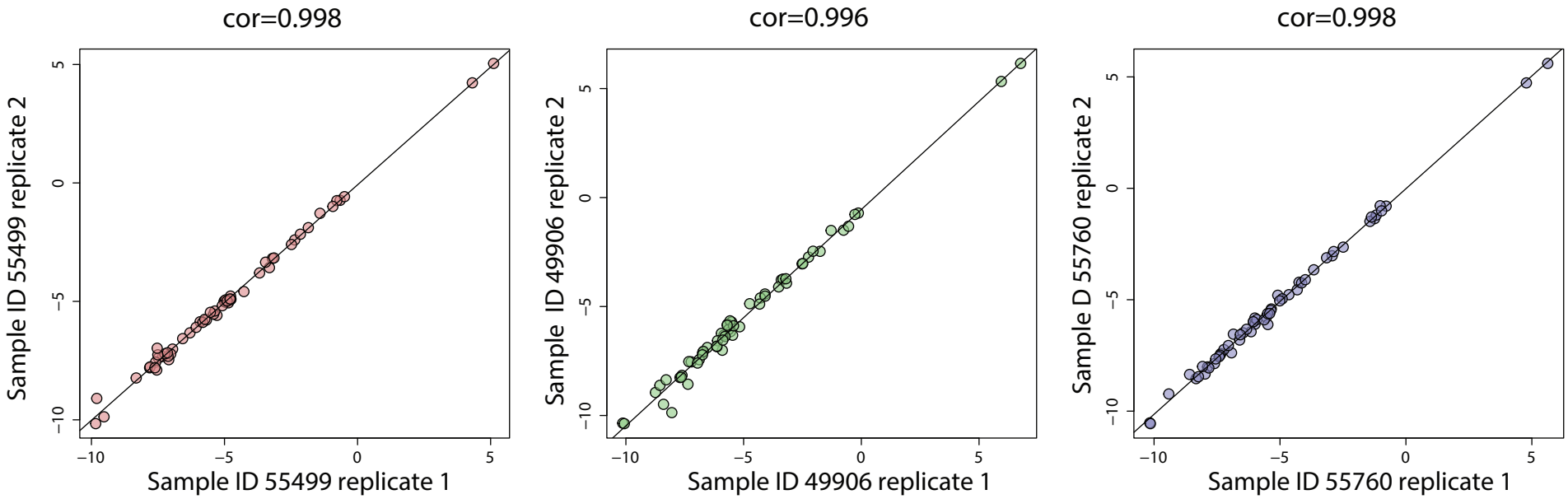
Supplemental Figure 3